

# High resolution photoemission spectroscopy study near the Fermi edge for different surfaces prepared on the icosahedral AIPdMn phase

T. Schaub<sup>1,a</sup>, J. Delahaye<sup>1</sup>, C. Berger<sup>1,b</sup>, H. Guyot<sup>1</sup>, R. Belkhou<sup>2</sup>, A. Taleb-Ibrahimi<sup>2</sup>, and Y. Calvayrac<sup>3</sup>

<sup>1</sup> Laboratoire d'Études des Propriétés Électroniques des Solides - CNRS, BP 166, 38042 Grenoble Cedex 9, France

<sup>2</sup> Laboratoire pour l'Utilisation du Rayonnement Électromagnétique, Université Paris Sud, 91405 Orsay Cedex, France

<sup>3</sup> Centre d'Études de Chimie Métallurgique - CNRS, 15 rue Georges Urbain, 94407 Vitry, France

Received 19 February 2000 and Received in final form 6 November 2000

**Abstract.** High resolution photoemission measurements performed at low temperatures on a single-grained sample of the AIPdMn icosahedral phase show that the density of states  $N(E)$  strongly depends on the nature of the surface. For an ordered quasicrystalline surface, prepared by Ar etching and ultra high vacuum annealing, a dip feature is observed in  $N(E)$  near the Fermi level, which energy dependence can be analyzed with a simple square-root power law. By contrast,  $N(E)$  varies only little with energy both for a disordered surface and a crystalline surface of the same sample. A sharp Fermi edge is then clearly observed. This shows that the metallic character of the surface of a quasicrystal is strongly reduced when the surface presents a quasicrystalline ordering.

**PACS.** 71.23.Ft Quasicrystals – 79.60.Bm Clean metal, semiconductor, and insulator surfaces – 71.55.Jv Disordered structures; amorphous and glassy solids

## 1 Introduction

Quasicrystals (QC) are highly ordered intermetallic compounds. Surprisingly, their electrical conductivity can be of the same order than that of semiconductor-based disordered systems lying on both sides of a metal-insulator transition [1,2]. An insulator is often defined by the existence of a gap in the electronic density of states  $N(E)$  at the Fermi level  $E_F$ , as it occurs in semiconductors. However, this doesn't include the case of Mott-Anderson insulators having a non vanishing  $N(E_F)$ , and where the insulating character is due to the localization of the wave function. A more general definition of an insulator is therefore that the zero temperature conductivity is zero. In QCs, there is actually no signature for a semiconductor type gap from bulk measurements, but there is a general agreement for a lower density of states at  $E_F$ , as compared to metals [1]. This is in general accordance with band structure calculations [3], and is often referred to as a Hume-Rothery mechanism. However there is no accurate determination of the depth of this pseudo-gap. The electronic depletion observed at  $E_F$  in soft X-ray spectroscopy studies [4] suffers from a limited energy resolution of  $\sim 0.1$ – $0.6$  eV. In specific heat the linear temperature-

term  $\gamma$ , which is reduced to about 1/4 of the expected free electron value [1] in the icosahedral phase *i*-AIPdMn, may include contributions from two-level tunneling states.

The energy dependence of  $N(E)$  close to  $E_F$  is also an essential information in order to understand the origin of the metal-insulator transition: opening of a true gap or Mott-Anderson type transition for instance. A sharp  $N(E)$  valley around  $E_F$  was inferred [5] from the anomalous temperature dependence of the spin-lattice relaxation time  $T_1$ . It could be of the order of a few 10 meV, *i.e.* much narrower than the Hume-Rothery pseudogap. This feature might be related to the prediction [3] of spiky structures in  $N(E)$  the width of which lies between a few 10 meV and a few 100 meV. However direct measurements of  $N(E)$  near  $E_F$  by photoemission spectroscopy on two differently prepared surfaces of the icosahedral *i*-AIPdMn phase (annealed [6] and scratched [7] respectively) have yielded contradictory interpretations. In the former case [6],  $N(E)$  decreases as  $\sqrt{E}$  close to  $E_F$  and the QC spectra, measured at room temperature, do not show a sharp Fermi edge. In contrast in the latter case [7],  $N(E)$  tends linearly towards an emphasized sharp Fermi edge (see also [8]).

One possible clue for these different photoemission results could be a difference in the effective thickness of material contributing to the spectra. The electronic structure can indeed be probed more or less deeply into the volume

<sup>a</sup> Now at SAP-AG.

<sup>b</sup> e-mail: berger@lepes.polycnrs-gre.fr

by tuning the energy of the incident photon beam. By comparing the photon energy used ( $h\nu = 13$  eV [6] and  $h\nu = 21.2$  eV [7]), it can be estimated that a thicker layer contributes to the spectra in the case of the annealed surface [6] as compared to the scratched (“metallic”) surfaces [7,8]. In fact, another study [9] has shown that the material could be more metallic at the top surface than deeper into the bulk in the case of an *i*-AlPdMn surface prepared by cleavage. However, even for a surface sensitive experiment (same photon energy as reference [7]) the distinct decrease of  $N(E)$  interpreted as a pseudogap was confirmed [10] for a QC surface annealed in similar conditions to reference [6]. Note that in that case, the depression near  $E_F$  is not observed by room temperature photoemission studies for a sputtered or a crystalline AlPdMn surface.

The aim of this article is to demonstrate that the nature of the surface itself is crucial for the poor metallicity at the surface of a quasicrystal. This requires high resolution experiments but also low temperatures since besides the improved resolution (which varies like  $4k_B T$ ), new phenomena can develop. By analyzing earlier results [11] of high resolution photoemission spectroscopy experiments at low temperature on a well characterized single grain of *i*-AlPdMn, we show that for a QC-surface annealed at high temperature the density of states has a strong variation near the Fermi level. This can be analyzed with a  $\sqrt{E}$  dependence. This dip is filled-in both for a disordered surface prepared by sputtering and for a crystalline surface of a different composition grown on top of the quasicrystal.

The paper is organized as follows. Section 2 presents the experimental set up and the surface preparation, Section 3, the results of photoemission for the three surfaces and the proposed analysis, and Section 4 is a discussion of the results.

## 2 Experimental set up and surface preparation

The single grain of *i*-AlPdMn was pulled out from the melt by the Czochralski method using a 5-fold axis quasicrystal-rod as a seed. This technique provides *i*-phases of very high structural quality [12]. The single grain of 11 mm diameter was homogenized for 120 hours at 1053 K. Its composition, measured by inductively coupled plasma emission spectrometry is Al-70.1  $\pm$  0.7, Pd-20.4  $\pm$  0.2 and Mn-9.5  $\pm$  0.08 at.%. No secondary phase (Al<sub>3</sub>Pd or decagonal phase) are detected with the synchrotron radiation. The sample was cut by spark erosion almost perpendicular to the 5-fold direction. It was mechanically polished to a mirror finish using a 1  $\mu$ m diamond paste at the final stage.

Measurements were done at the high resolution beamline SU3 of the superACO (LURE) synchrotron ring. Experiments were performed below  $1 \times 10^{-10}$  mbar, using a VSW-150 hemispherical analyzer. The best resolution delta (analyser + photons) was about 20 meV, yielding a total broadening of  $\approx 32$  meV at the lowest temperature *i.e.* 40 K. Cycles of Ar<sup>+</sup> sputtering ( $7 \mu\text{Acm}^{-2}$  at 1.5 keV)

were performed before annealing (up to 870 K) and also while annealing the sample (up to 570 K). The temperature was recorded by a thermocouple fixed on the sample holder next to the surface. The cycles were repeated until no trace of alumina could be detected in the Al  $2p$  spectra using the low photon energy of the synchrotron light or at high photon energy of an X-ray source (Mg K $_{\alpha}$ ). Three different surfaces were prepared: quasicrystalline (QC), crystallized and disordered.

The QC-surface was obtained after sputtering-annealing cycles [13] at 700 K. The Mn  $2p_{3/2}$  core level line at 641 eV binding energy then had a narrow symmetrical profile. In metals the asymmetry parameter originates from intrinsic energy losses through the excitation of electron-hole pairs and it is therefore related to the absolute value of the electronic density of states at  $E_F$ . The symmetry of the core level thus indicates a low  $N(E_F)$  for such a prepared surface. This property was previously used as an indicator of the presence of the QC-order at the surface [14,15]. After annealing, a characteristic five-fold symmetry LEED pattern was observed at electron energy of 60 eV with its spots sharpening after repeated cycles.

After sputtering and annealing at temperatures below 670 K, a crystalline surface phase was grown on top of the single grain. Its composition was estimated elsewhere [16] to be approximately Al<sub>50</sub>Pd<sub>40</sub>Mn<sub>10</sub>. We have observed the characteristic ten-fold symmetric LEED pattern of this phase, which has been explained by five different orientations of a cubic crystal with its [110] symmetry axis parallel to a five-fold axis of the underlying *i*-phase [16].

The disordered surface was prepared by a short time (1 minute) sputtering of the well prepared QC-surface. Contrary to the QC-surface, the Mn  $2p_{3/2}$  core level measured under the same conditions was asymmetric, which is a first evidence of a more metallic state. We expect that the sputtering was slight enough not to induce significant compositional changes. Indeed, a dramatic change was observed [17] in the surface composition of a *i*-AlPdMn single grain after sputtering by Ar at 3 kV: the Al composition drops from about 72 at.% down to about 50 at.% for a fluency of  $30 \times 10^{15}$  ions/cm<sup>2</sup>. For the fluency we used (about  $1.5 \times 10^{15}$  ions/cm<sup>2</sup>), at most a few percent reduction in Al would be expected at 3 kV. To check this point, we have measured the areas of the Al  $2p$  core levels at 72 eV before and immediately after having sputtered the well ordered QC-surface, for Al is the most subjected to depletion by Ar<sup>+</sup> etching. The spectra were taken at photon energy  $h\nu = 100$  eV, which corresponds to a photoelectron kinetic energy of  $E_c \approx 25$  eV and an electron escape depth of  $\lambda \approx 5$  to 6 Å. As seen in Figure 1, both areas are the same, and we thus could not detect a change of composition at the surface - within the probing depth  $\lambda$ . The structure of the disordered surface was not further characterized. In the following, the ultra violet photoemission curves close to the Fermi level are recorded with similar electron kinetic energy, *i.e.* probing the same surface thickness.

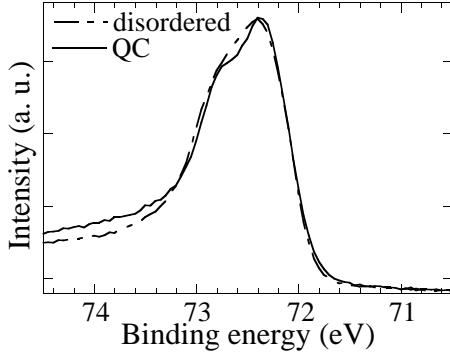


**Fig. 1.** Al 2*p* core level line for photons of  $h\nu = 100$  eV. The Al 2*p* spin splitting, clearly resolved for the QC-surface, is evidently lost for the disordered surface.

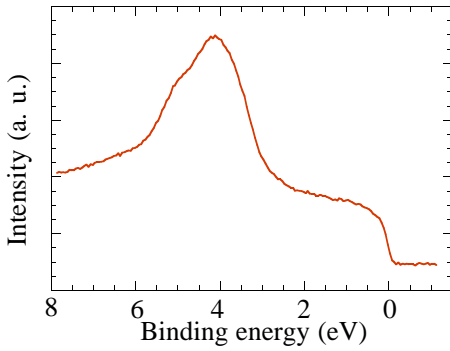


**Fig. 2.** Room temperature energy distribution curve for the QC surface (photon energy  $h\nu = 40$  eV, experimental resolution  $\delta = 70$  meV).

### 3 Results

#### 3.1 EDC of the QC, crystalline and disordered surfaces

The photoelectron Energy Distribution Curve (EDC) of Figure 2, taken at room temperature, presents the valence band of the QC-surface. The main peak at binding energy  $E \approx 4$  eV is attributed to Pd 4*d* states [18]. The shoulder at 5 eV is ascribed to the 4*d* spin splitting [18]. The states below the Fermi level are believed to originate from the Mn 3*d* states [4,19]. Note that we could not detect the dispersing peak observed in reference [6] at a binding energy of about 2 eV.

Figure 3 shows the low temperature normalized EDC near  $E_F$  obtained for the three surfaces with photon energies of 13 eV or 17 eV (kinetic energy  $E_c \approx 9$  and 13 eV respectively for electrons at  $E_F$ , *i.e.* escape depth  $\approx 10$  Å). Each spectrum is compared to a reference metal spectrum (Molybdenum plate) taken within a few minutes interval, to make sure of similar experimental conditions. The actual temperature of the surface was determined by fitting the Mo spectrum by a step function convoluted by a Gaussian function of width at half maximum  $\Delta = \delta + 4k_B T$  ( $\delta = 20$  meV) once subtracted a polynomial background which is believed to originate mainly from harmonic contributions of the synchrotron radiation. For a metal near  $E_F$ , this fit takes into account the thermal broadening of

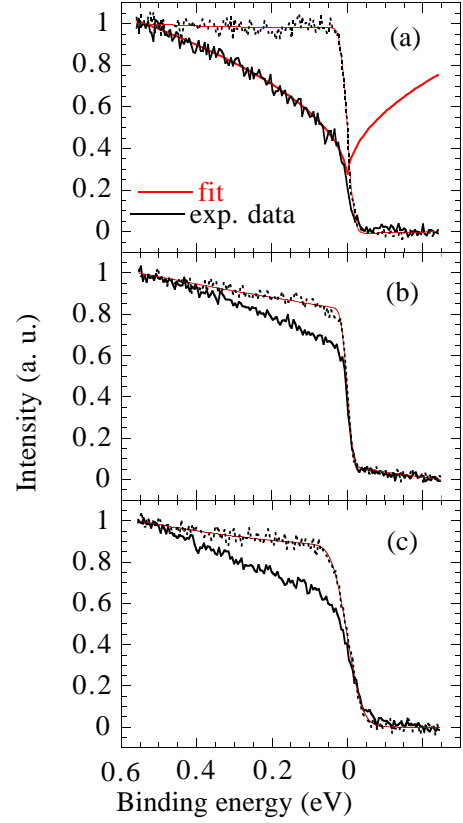


**Fig. 3.** High resolution ( $\delta = 20$  meV) EDC for three surface states: (a) QC ( $T = 40$  K,  $h\nu = 17$  eV), (b) disordered ( $T = 30$  K,  $h\nu = 13$  eV) and (c) crystalline ( $T = 160$  K,  $h\nu = 13$  eV) in comparison to Mo metal under the same conditions (broken line). The full lines are fits as explained in the text.

the Fermi distribution. It also provides the reference position of  $E_F$ .

In this energy range (binding energy  $E_B < 550$  meV), it is readily observed that the EDC of the QC-surface is quite different from that of the reference metal: it drops smoothly towards  $E_F$ . In the normalized unit of Figure 3, the EDC value is reduced by more than half its value at 550 meV before the Fermi cut-off, whereas in the Mo metal reference, the EDC reduction seen in Figure 3 is entirely due to the Fermi cut off. For the disordered and crystalline surfaces, the EDCs have a less pronounced difference with the reference metal, since they vary little in energy towards a more clearly visible sharp edge at  $E_F$ . Also the EDCs are clearly enhanced compared to the one of the QC-surface, thus indicating a more metallic character than for the QC-surface. At room temperature (see Fig. 4), the EDCs for the three surfaces are much closer to one another but can still be distinguished despite the fact that the spectral width at the Fermi edge is dominated here by the thermal broadening.

#### 3.2 Analysis of the QC-surface

In order to evaluate the spectral function of  $N(E)$  at low temperature, we have here restricted our analysis to

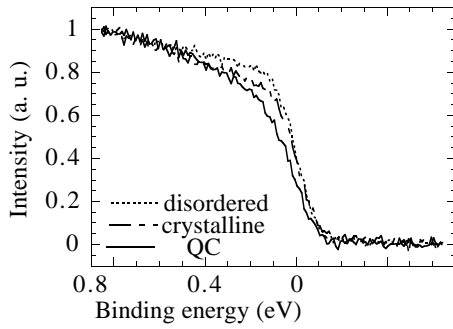


**Fig. 4.** ECD for the QC, crystalline and disordered surfaces at room temperature ( $h\nu = 40$  eV,  $\delta = 70$  meV).

binding energies  $E \geq \delta + 4k_B T$ , *i.e.* in a range where the EDC reflects  $N(E)$  smoothed at the scale of  $\delta$ , and  $E \leq 550$  meV, *i.e.* not too far from  $E_F$  (see below). We have chosen a power law as a test function to fit the data, which is the simplest as possible energy dependence. The reason for this is that we have previously measured a single  $\sqrt{E}$  centered at  $E_F$  by tunneling spectroscopic measurements [23]. Also such a law is expected close to  $E_F$  in the one electron density of states from the analogy of the AlPdMn quasicrystal with disordered systems close to the metal-insulator transition [1]. Moreover, from a completely different physical origin, a  $\sqrt{E}$  dependence is also derived from Van-Hove singularities in  $N(E)$  as outlined in reference [6]. By taking into account a linear background, the EDC for the QC-surface could be well fitted by  $N_{QC}(E) = a + b|E|^\alpha$  for  $\delta + 4k_B T = 33$  meV  $\leq E \leq 550$  meV. At somewhat higher binding energies the EDC is essentially flat. In the normalized units of Figure 3a, we obtained  $a = 0.25 \pm 0.05$ ,  $b = 1 \pm 0.05$ ,  $\alpha = 0.46 \pm 0.05$ . The same values were obtained by fitting the EDC of the same surface measured at 70 K with a much longer acquisition time, and with  $h\nu = 13$  eV, *i.e.* slightly less surface sensitive. The EDC is shown in Figure 5. Therefore, the density of states  $N_{QC}(E)$  at low temperature can be analyzed by a  $\sqrt{E}$  term, of characteristic energy  $(a/b)^2 \approx 60$  meV, plus a constant term reflecting the remaining states at  $E_F$  (25% of the states at 0.55 eV). At room temperature, the accuracy of the fit is much poorer, due to phonon broadening, but a significant  $N_{QC}(E)$  reduction is also present.

The same analysis performed for the crystalline and disordered surfaces at low temperature yielded  $\alpha \approx 1$  and larger values of  $a$  ( $a \approx 0.7$ ). Such a linear dependence with energy is however hardly distinguishable from a constant  $N(E)$  once subtracted a linear background, like the one found for Mo metal. In order to obtain a more quantitative comparison between the QC surface and the disordered surface, we have normalized the valence bands to the Pd  $4d$  peak at 4 eV. Both EDCs then happen to have the same value on the plateau around  $E_B \approx 1$  eV, which is a further confirmation of the reduction of the absolute value of  $N(E_F)$  in the QC-surface compared to the disordered one.

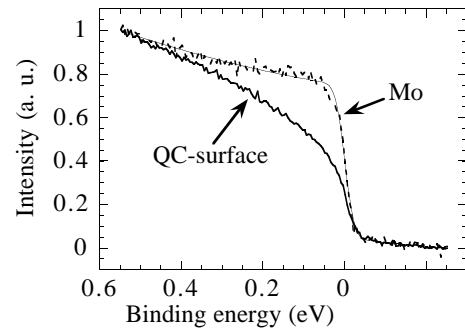


**Fig. 5.** ECD for the QC-surface at 70 K ( $h\nu = 13$  eV,  $\delta = 20$  meV).

So we can conclude to the absence of the dip feature for both the crystalline and disordered surfaces. In both cases,  $N(E)$  varies slightly with  $E$  and has a higher value at  $E_F$  than  $N_{QC}(E_F)$ . This is in accordance with the higher electrical conductivity in disorder *i*-AlPdMn phases [20]. For the comparison with the crystalline surface, it will be difficult to separate the relative effects of a different structural or chemical order. We note that similar EDCs than the one observed in Figure 4 have been recently reported [10] by photoemission technique at room temperature on similarly prepared surfaces (sputtered, QC and crystalline). Note however that in that case the  $\sqrt{E}$  dependence was claimed not to be developed at variance with our low temperature measurement.

## 4 Discussion

### 4.1 Electronic density of states at $E_F$

Before discussing the results, we recall that cycles of Ar etching and annealing were shown to restore an ordered QC-surface, which was described as a bulk terminated surface [13,21]. So we could expect the photoelectron spectra of our QC-surface, which are sensitive to several atomic layers, to reflect, at least partly, that of the bulk.

We now comment about the value of  $N(E)$  at  $E_F$ . We have determined that even for the QC-surface there remain states at  $E_F$  with a much lower density than at higher binding energy (about 1/4 the value at 550 meV). This was expected from bulk measurements yielding a conductivity on the metallic side of the metal-insulator transition, and a low linear  $T$ -term  $\gamma$  (but non zero) of the specific heat [1]. This result for  $N_{QC}(E_F)$  is to be compared with the analysis [6] of angular-resolved photoemission studies at room temperature on an *i*-AlPdMn single grain. It indicates a vanishing  $N(E)$  at  $E_F$ , although a precise determination could not be achieved due to the limited resolution at room temperature. The absence of a sharp Fermi edge has suggested [6] a pseudogap has opened at  $E_F$  like in semimetals. Our observed  $N_{QC}(E)$  also differs from the spectra, also taken a low temperature, on diamond scratched surfaces [7]. This is readily seen from the figures and confirmed by the model dip of reference [7] giving  $N(E_F) \approx 3/4$  the value at 550 meV

(from Fig. 4 of Ref. [7]), with an overall feature quite comparable to our disordered or crystalline surfaces.

## 4.2 Spectral function of $N_{\text{QC}}(E)$

Now concerning the energy dependence of  $N(E)$ , we have determined that  $N_{\text{QC}}(E)$  can be well fitted by a  $\sqrt{E}$  power law close to  $E_{\text{F}}$  (from 33 to 550 meV below  $E_{\text{F}}$ ). In agreement with all published photoemission data, the fine structures predicted for approximant phases [3] are not observed here, although the widest peaks should be resolved with the present resolution. The observed  $\sqrt{E}$  power law is in general agreement with the analysis of reference [6]. But our findings are in contrast with the observation of EDCs depending weakly and linearly on energy on scratched surfaces [7].

Note that the enhanced metallic  $N(E)$  deduced from the Al  $2p$  core level analysis [9] at the very surface of a cleaved *i*-AlPdMn single grain corresponds to a surface order consisting of clusters [22] instead of the flat terraces that can develop with high temperature annealing [13].

The  $\sqrt{E}$  law of  $N_{\text{QC}}(E)$ , is comparable to the one found in tunneling conductivity  $dI/dV(V)$  spectra [23]. In the standard approximation  $dI/dV(V)$  is proportional to the density of states  $N(E)$  at the energy  $E$  given by the voltage  $V$  ( $E = eV$ ). The tunneling spectra are taken at 4 K, in the voltage range  $\pm 300$  mV. At higher voltage spurious effects can be observed due to the barrier. In the same energy and temperature range as the photoemission curves, we have found  $dI/dV = a + b\sqrt{|V|}$ . This corresponds to an energy dip of  $(a/b)^2 \approx 10 - 100$  meV, of width comparable to the analyze of the present EDCs. Note that a narrow  $\sqrt{E}$  dip in  $N(E)$  was also claimed to account for the temperature dependence of the nuclear relaxation time  $T_1$  measured by NMR [5] in *i*-AlCuFe.

The  $\sqrt{E}$  dependence may arise from different physical mechanisms. In reference [6], it was ascribed to Van-Hove singularities, which occur at  $k$  points where the dispersion relation  $E(k)$  is flat. Flat bands are indeed expected in QCs close to  $E_{\text{F}}$  from the Hume-Rothery mechanism, and are predicted by band structure calculations in approximant phases [3]. However, one would have expected several singularities, not only that close to  $E_{\text{F}}$ .

Another possibility is the square root anomaly which deepens around  $E_{\text{F}}$  at low temperature in the one electron density of states for disordered systems on the metallic side near to a metal-insulator transition. It originates from electron-electron interactions in the strongly diffusive regime. These quantum corrections have been unambiguously observed by electronic transport measurements in *i*-AlPdMn [1]. It is worth noting that in that case a single dip centered at  $E_{\text{F}}$  is expected, with a narrow energy width, in accordance with the typical energy range where it is observed in the present photoemission study. Assuming that photoemission spectroscopy measures the same quantity as tunneling spectroscopy, namely the one electron density of states [24], it is therefore not so surprising not to observed the predicted spicky structure [3].

Indeed electron-electron interactions are poorly taken into account in these calculations.

Both interpretations (electron-electron interactions and Van-Hove singularities) lead to an erasure of the dip structure in the density of states as a result of disorder. First, any structure of  $N(E)$  will be smoothed out on a scale  $\hbar/\tau$  ( $\tau$  is the scattering time). Second, as disorder in general enhances the conductivity of QC phases, it should lower the effects of electron-electron interaction on  $N(E)$ .

## 4.3 Extrinsic losses

The previous analysis was based on the usual assumption that the EDC reflects  $N(E)$ . However, Joynt [25] very recently showed that extrinsic ohmic losses suffered by a photoelectron after being emitted from the solid can mimic pseudogap effects in the EDC, although there is no variation in the underlying  $N(E)$ . These losses are expected to be important in materials with low conductivity, albeit not all of them [26], and having a significant absorptive part of the conductivity at the relevant frequency. This is precisely the case of our QC sample (see [1] and optical conductivity measurements in [27]). We emphasize that this other interpretation would yield the same conclusion on a less metallic surface for the QC-surface in comparison to the disordered and crystalline ones. Indeed, from Joynt's model, for a constant  $N(E)$  the lower the conductivity the stronger the pseudogap feature. In this model, the inelastic part of the spectrum is inversely proportional to the speed of the outgoing electron. Then, to be genuine, a pseudogap must be present in the EDC for all incident photon energies, assuming that  $N(E)$  is not too much affected by the photoelectron escape depth. Another test for a pseudogap to be real could be provided by the angular-dependence of the EDC since the losses are momentum-independent, while in general the pseudogap is not. In a quasicrystal the angular dependence of the EDC will thus be an interesting issue [28].

## 5 Summary

In summary, we have studied by high resolution photoemission spectroscopy at low temperature the electronic density of states close to the Fermi level of *i*-AlPdMn surfaces. The QC-surface, characterized by a five-fold LEED pattern and a narrow and symmetrical Mn  $2p_{3/2}$  profile, presents a narrow  $\sqrt{E}$  dip feature which is well developed at low temperature. This compares well with tunneling spectroscopy in the same temperature and energy range, where the  $\sqrt{E}$  depression can be attributed to electron-electron interaction effects. By contrast, for a disordered surface, this feature is filled-in, with a linear  $N(E)$  towards a much more developed Fermi edge. The same trend is observed for a crystalline surface grown on top of the *i*-sample. We thus have established that the metallic character of the surface of an *i*-phase is strongly reduced for

a quasicrystalline surface ordering. The fact that the electronic surface properties of *i*-phases are severely affected by surface preparation could have consequences for specific properties of QCs such as low friction and low surface energy, which are the leading properties for industrial applications.

We would like to thank P. Thiel and J. Chevrier for their advice in surface preparation, T. Grenet and D. Mayou for fruitful and stimulating discussions.

## References

1. S.J. Poon, *Adv. Phys.* **41**, 303 (1992); C. Berger, T. Grenet, *From Quasicrystals to More Complex Systems* (EDP Sciences, Les Ulis, 2000) p. 49; T. Grenet, *Current Topics in Quasicrystals*, edited by E. Belin-Ferré, C. Berger, M. Quiquandon, A. Sadoc (World Sci., Singapore, 2000) p. 455.
2. F.S. Pierce, S.J. Poon, Q. Guo, *Science* **261**, 737 (1993); J. Delahaye, J.-P. Brison, C. Berger, *Phys. Rev. Lett.* **81**, 4204 (1998); M. Rodmar, M. Ahlgren, D. Oberschmidt, C. Gignoux, J. Delahaye, C. Berger, S.J. Poon, Ö. Rapp, *Phys. Rev. B* **61**, 3936 (2000).
3. G. Trambly de Laissardière, T. Fujiwara, *Phys. Rev. B* **50**, 5999 (1994); M. Krajčí, M. Windisch, J. Hafner, G. Kresse, M. Mihalkovič, *Phys. Rev. B* **51**, 17 355 (1995).
4. E. Belin, Z. Dankhazi, A. Sadoc, J.-M. Dubois, *J. Phys. Cond. Matt.* **6**, 8771 (1994).
5. X.-P. Tang, E.A. Hill, S.K. Wonnell, S.J. Poon, Y. Wu, *Phys. Rev. Lett.* **79**, 1070 (1997); Simonet *et al.*, *Quasicrystals*, edited by S. Takeuchi, T. Fujiwara (World Sci., Singapore, 1998) p. 696.
6. X. Wu, S.W. Kycia, C.G. Olson, P.J. Benning, A.I. Goldman, D.W. Lynch, *Phys. Rev. Lett.* **75**, 4540 (1995).
7. Z.M. Stadnik, D. Purdie, M. Garnier, Y. Baer, A.-P. Tsai, A. Inoue, K. Edagawa, S. Takeuchi, *Phys. Rev. Lett.* **77**, 1777 (1996).
8. Z.M. Stadnik *et al.*, *Phys. Rev. B* **55**, 10938 (1997).
9. G. Neuhold, S.R. Barman, K. Horn, W. Theis, Ph. Ebert, K. Urban, *Phys. Rev. B* **58**, 734 (1998).
10. D. Naumović, P. Aebi, L. Schlapbach, C. Beeli, T.A. Lograsso, D.W. Delaney, *Phys. Rev. B* **60**, R16330 (1999).
11. J. Delahaye, C. Berger, T. Grenet, T. Schaub, H. Guyot, J.P. Brison, A. Taleb-Ibrahimi, R. Belkhou, *Int. Conf. Moriond: Physics at mesoscopic scale, Les Arcs, jan. 1999* (Éditions Frontières, to appear).
12. for instance: M.J. Capitan *et al.*, *Quasicrystals*, edited by C. Janot, R. Mosseri (World Sci., Singapore, 1995) p. 652.
13. T.M. Schaub, D.E. Bürgler, H.-J. Güntherodt, J.B. Suck, *Phys. Rev. Lett.* **73**, 1255 (1994).
14. C.J. Jenks, S.-L. Chang, J.W. Andereg, P.A. Thiel, *Phys. Rev. B* **54**, 6301 (1996).
15. V. Fournée, P.J. Pinhero, J.W. Andereg, T.A. Lograsso, A.R. Ross, P.C. Canfield, I.R. Fisher, P.A. Thiel, *Phys. Rev. B* **62**, 14049 (2000).
16. Z. Shen *et al.* *Phys. Rev. B* **58**, 9961 (1998); B. Bolliger *et al.* *Phys. Rev. Lett.* **80**, 5369 (1998). D. Naumović *et al.*, *Quasicrystals*, edited by S. Takeuchi, T. Fujiwara (World Sci., Singapore, 1998) p. 749.
17. C.J. Jenks, J.W. Burnett, D.W. Delaney, T.A. Lograsso, P.A. Thiel, *Appl. Surf. Sci.* **157**, 23 (2000).
18. S. Hüfner, *Spring. Ser. Solid-State Sci.* **82**, (1995).
19. G.W. Zhang, Z.M. Stadnik, A.-P. Tsai, A. Inoue, *Phys. Letters A* **186**, 345 (1994).
20. D. Mayou, *Phys. Rev. Lett.* **70**, 3915 (1993); see also: R. Haberkern, *et al. Quasicrystals*, edited by S. Takeuchi, T. Fujiwara (World Sci., Singapore, 1998) p. 643.
21. M. Gierer *et al.* *Phys. Rev. B* **57**, 7628 (1998); D. Naumović, P. Aebi, L. Schlapbach, C. Beeli, *New Horizon in Quasicrystals*, edited by A.I. Goldman *et al.* (World Sci., Singapore, 1997) p. 86; J. Alvarez, Y. Calvayrac, J.L. Joulaud, M.J. Capitan, *Surf. Sci.* **423**, L251 (1999).
22. Ph. Ebert, M. Feurbacher, N. Tamura, M. Wollgarten, K. Urban, *Phys. Rev. Lett.* **77**, 3827 (1996).
23. Davydov D.N. *et al.*, *Phys. Rev. Lett.* **77**, 3173 (1996); J. Delahaye, T. Schaub, C. Berger (unpublished).
24. J. Imry, private communication.
25. R. Joynt, *Science* **284**, 777 (1999).
26. D.S. Dessau, T. Saitoh, *Science* **287**, 767a (2000).
27. L. Degiorgi, M.A. Chernikov, C. Beeli, H.R. Ott, *Solid State Comm.* **87**, 721 (1993).
28. E. Rotenberg, W. Theis, K. Horn, P. Gille, *Nature* **406**, 602 (2000).